Autoimmunity Reviews 15 (2016) 577–584

Contents lists available at ScienceDirect

Autoimmunity Reviews

journal homepage: www.elsevier.com/locate/autrev

Review

A novel method for high-throughput detection and quantification of neutrophil extracellular traps reveals ROS-independent NET release with immune complexes

Tineke Kraaij [a], Fredrik C. Tengström [a], Sylvia W.A. Kamerling [a], Charles D. Pusey [b], H. Ulrich Scherer [c], Rene E.M. Toes [c], Ton J. Rabelink [a], Cees van Kooten [a], Y.K. Onno Teng [a,*]

[a] Department of Nephrology, Leiden University Medical Center, Albinusdreef 2, 2333 ZA Leiden, The Netherlands
[b] Department of Medicine, Renal and Vascular Inflammation Section, Imperial College London, United Kingdom
[c] Department of Rheumatology, Leiden University Medical Center, Albinusdreef 2, 2333 ZA Leiden, The Netherlands

ARTICLE INFO

Article history:
Received 13 February 2016
Accepted 15 February 2016
Available online 27 February 2016

Keywords:
Neutrophils
Neutrophil extracellular traps
Autoimmune disease

ABSTRACT

A newly-described first-line immune defence mechanism of neutrophils is the release of neutrophil extracellular traps (NETs). Immune complexes (ICxs) induce low level NET release. As such, the in vitro quantification of NETs is challenging with current methodologies. In order to investigate the role of NET release in ICx-mediated autoimmune diseases, we developed a highly sensitive and automated method for quantification of NETs. After labelling human neutrophils with PKH26 and extracellular DNA with Sytox green, cells are fixed and automatically imaged with 3-dimensional confocal laser scanning microscopy (3D-CLSM). NET release is then quantified with digital image analysis whereby the NET amount (Sytox green area) is corrected for the number of imaged neutrophils (PKH26 area). A high sensitivity of the assay is achieved by a) significantly augmenting the area of the well imaged (11%) as compared to conventional assays (0.5%) and b) using a 3D imaging technique for optimal capture of NETs, which are topologically superimposed on neutrophils. In this assay, we confirmed low levels of NET release upon human ICx stimulation which were positive for citrullinated histones and neutrophil elastase. In contrast to PMA-induced NET release, ICx-induced NET release was unchanged when co-incubated with diphenyleneiodonium (DPI). We were able to quantify NET release upon stimulation with serum from RA and SLE patients, which was not observed with normal human serum. To our knowledge, this is the first semi-automated assay capable of sensitive detection and quantification of NET release at a low threshold by using 3D CLSM. The assay is applicable in a high-throughput manner and allows the in vitro analysis of NET release in ICx-mediated autoimmune diseases.

Contents

* Corresponding author at: Leiden University Medical Center, Department of Nephrology, C7, 2333 ZA Leiden, The Netherlands. Tel.: +31 715262148; fax: +31 715266868.
E-mail addresses: t.kraaij@lumc.nl (T. Kraaij), C.F.Tengstroem@lumc.nl (F.C. Tengström), s.w.a.kamerling@lumc.nl (S.W.A. Kamerling), c.pusey@imperial.ac.uk (C.D. Pusey), H.U.Scherer@lumc.nl (H.U. Scherer), R.E.M.Toes@lumc.nl (R.E.M. Toes), a.j.rabelink@lumc.nl (T.J. Rabelink), C.van_Kooten@lumc.nl (C. van Kooten), y.k.o.teng@lumc.nl (Y.K.O. Teng).

http://dx.doi.org/10.1016/j.autrev.2016.02.018

1. Introduction

Neutrophil extracellular traps (NETs) are extracellular strands of DNA that are expulsed upon the interaction of neutrophils with infectious pathogens such as *Staphylococcus aureus* [1], *Salmonella typhi*, *Shigella flexneri* [2], *Candida albicans* [3] and *Aspergillus fumigatus* [4]. The extracellular NET fibres were demonstrated to be composed of nuclear chromatin, citrullinated histones and multiple granular antimicrobial and cytoplasmic proteins like myeloperoxidase (MPO) and neutrophil elastase (NE) [2]. The physiological function of NETs is the entrapment and subsequent elimination of these pathogens. NETs are therefore considered as part of a first line defence mechanism and, as such, the antimicrobial armamentarium of neutrophils consists of phagocytosis, degranulation of lysozymes and extrusion of NETs.

The discovery of NETs as a source of extracellular DNA has triggered several investigations to study its role in autoimmune diseases (AIDs), because extracellular DNA is an established trigger of autoimmunity [5]. NETs are postulated to have a potentially pathogenic role in ANCA-associated small-vessel vasculitis [6,7], systemic lupus erythematosus [8,9] and rheumatoid arthritis [10]. Moreover, reduced degradation of NETs was associated with more severe disease in AID patients [11,12]. Because almost any pathogen can induce NET formation, it seems unlikely that in light of the many (subclinical) microbial attacks that humans continuously face, every 'infection' also potentially induces an autoimmune response. Therefore, it is relevant to identify non-infectious triggers of NET formation which contribute to increased NETosis as underpinning pathogenic mechanisms of autoimmunity.

To address the issue of NET-inducing triggers, current studies are hampered by the lack of a reliable and sensitive quantification method of NET formation. In contrast to PMA-induced NETosis which usually leads to an overwhelming extrusion of DNA, physiological stimuli like immune complexes (ICxs)) induce more subtle and lower levels of NET formation [13]. Currently, two methods are commonly used to quantify NET release in vitro: DNA measurements in supernatant [7,8,14] or demonstration of extracellular DNA by immunocytochemistry [6,15–17]. With respect to the first method, DNA measurements are straightforward and objective but not specific for NETs. Also, several molecules, most importantly immunoglobulins, can interfere with fluorescence measurements [18]. With respect to the second method, quantification based on immunocytochemistry is heterogeneously reported by number of netting neutrophils, neutrophils with decondensed nuclei or area of extracellular DNA after image analysis. This method is prone to subjectivity of the observer and is quite labour intensive. Therefore, the aim of the present study was to develop a highly sensitive, objective and reproducible NET quantification assay applicable in a high-throughput system. Here, we describe how ICx-induced NET formation is sensitively detected and quantified by a semi-automated, confocal laser scanning microscopy (CLSM) 3D-imaging technique.

2. Methods

2.1. Patient samples

All serum samples were obtained after informed consent. Peripheral blood was obtained without anticoagulants and serum samples were stored at −80 until use. Twenty-seven rheumatoid arthritis (RA) and 20 systemic lupus erythematosus (SLE) serum samples were collected. Six normal human serum (NHS) samples, acquired from a healthy donor bank, were used as a control. 10% serum was used in the assay and each sample was tested in triplicate within one experiment.

2.2. Preparation of neutrophils

Twenty millilitres of whole blood was collected in EDTA-coated tubes. Neutrophils were isolated by density gradient centrifugation with Ficoll-amidotrizoaat (LUMC, Leiden, The Netherlands) followed by erythrocyte lysis. Cells were counted using trypan blue, labelled with PKH26 (2 μM, Sigma-Aldrich, Saint-Louis, MO, USA) and then 3.75×10^4 neutrophils were seeded per well into a 96-well culture plate in a phenol red-free RPMI 1640 medium (Life Technologies, The Netherlands) supplemented with 2% heat-inactivated foetal calf serum (FCS). Neutrophils were stimulated during 3:45 h with any given stimulus. Stimuli used were medium (negative control), intravenous immunoglobulins (IVIG) (Nanogam 50 mg/mL; Sanquin, Amsterdam, The Netherlands), purified IgG, heat-aggregated IgG immune complexes or phorbol myristate acetate (PMA) (Sigma-Aldrich). For NADPH oxidase inhibition, 1 μM diphenyleneiodonium (DPI) (Sigma-Aldrich) was used. Hereafter, an impermeable DNA dye, 1 μM Sytox green (Life Technologies), was added for 15 min after which neutrophils were fixed with 4% formaldehyde (Added Pharma).

2.3. Fluorescence immunocytochemistry of NETs

PKH-labelled neutrophils were seeded onto poly-D-lysine-coated coverslips (Corning, NY, USA) and NETs were induced according to the abovementioned protocol. Fixed neutrophils were blocked with 1% BSA and 5% normal goat serum in PBS and stained with polyclonal rabbit anti-human citrullinated histon3 (10 μg/ml, Abcam) or a mouse monoclonal anti-human citrullinated histon3 (10 μg/ml, Abcam) and polyclonal rabbit neutrophil elastase (NE) (10 μg/ml, Abcam) in PBS and incubated for 2 h. Then, neutrophils were washed and incubated with a 1/500 dilution secondary goat anti-rabbit Alexa488 antibody (Life Technologies) or with a 1/500 dilution secondary goat anti-mouse Alexa488 antibody (Life Technologies). The secondary antibodies were pre-incubated for 30 min with 10% normal human serum to bind anti-human immunoglobulins. After 60 min incubation, neutrophils were washed and stained with Hoechst 33258 (1 μg/ml, Life Technologies). Images were acquired with the Leica DMI6000 inverted microscope using a 20× magnification.

2.4. Preparation of heat-aggregated IgG immune complexes

IgG was enriched from pooled healthy human sera by the use of a diethylaminoethyl (DEAE) cellulose anion exchange column (GE Healthcare) [19]. Samples were centrifuged over the DEAE column and subsequently the column was flushed with TRIS buffer. The eluate containing IgG was concentrated with a centrifugal filter unit with a cut-off at 30 kDa (Merck Millipore). IgG enrichment was confirmed with SDS-polyacrylamide gel electrophoresis (10% Mini-Protean TGX gel, Biorad). Briefly, the precast gel was run with non-reduced and reduced samples (reducing agent DTT, New England Biolabd) at 30 mA at room temperature. Bands were detected with Coomassie Brilliant Blue protein staining (Biorad). The obtained IgG was aggregated by heating in a water bath at 63° for 20 min at a concentration of 25 mg/ml. Then, the solution was

centrifuged at 3000 rpm for 10 min and the supernatant, containing the aggregates, was loaded on a Sepharose 4B column (GE Healthcare) for fractionation of the IgG aggregates. A solution of monomeric IgG was used as a standard. Large aggregates, consisting of more than 40 IgG monomers, were collected to use in the confocal laser scanning microscopy (CLSM) NET assay. Monomeric IgG was used as a control. The IgG concentration was defined with a Pierce assay.

2.5. Visualization of neutrophil extracellular traps

Immediately following fixation, neutrophil extracellular traps (NETs) were visualized by confocal laser scanning microscopy (CLSM) using the automated BD Pathway 855 (BD Biosciences, San Jose, CA, USA). Briefly, 12 z-stacked images of 25 predefined high power fields (HPFs) at a 20× magnification were captured. The HPFs were evenly spread throughout the well by a standardized 5 × 5 zig-zag pattern with 400 μm (length) and 500 μm (width) spaced between each high HPF.

The well area covered by the above-described microscopic imaging was calculated as follows: 1) the area of a HPF at a 20× magnification was calculated at $3.3 * 10^6$ μm^2 (length 417.39 μm × width 318.01 μm); 2) the area of a HPF at a 40× magnification was calculated at $0.8 * 10^6$ μm^2 (length 210.49 μm × width 160.38 μm); 3) total area covered was calculated by multiplying the number of HPFs by the HPF-area at a given magnification. The microscope was programmed to automatically focus on PKH26 membrane staining. Then, for each image PKH26 (Cy3) and Sytox green (alexa488) were visualized. The CLSM exposure time for Sytox green was set on the positive control and for PKH26 on the negative control. The same exposure time was applied to all images in the same experiment.

2.6. Automatic digital image analysis for the quantification of NET formation

Acquired images were automatically analysed by ImageJ image analysis software (NIH, Bethesda, MD, USA). Extracellular DNA of NETs was quantified as the cumulative area of positive Sytox green. To correct for the number of neutrophils, the mean area of positive PKH26 staining was quantified. Thus, the ratio of both areas is calculated, representing the NET area corrected for the amount of imaged neutrophils in each sample. A higher ratio indicates a larger NET area present.

3. Results

3.1. NETs are induced at lower levels by human immune complexes as compared to PMA

Immune complexes are considered as pathogenic compounds in human autoimmune diseases and capable of inducing NETs [20,21]. We first confirmed that human heat-aggregated IgG ICx indeed induced NET formation. Extracellular DNA was detected by immunofluorescence and we confirmed that the extracellular DNA was positive for citrullinated histones (citH3) and neutrophil elastase (NE) (Fig. 1A, B). Visually, ICx induced NET release at much lower levels compared to PMA (Fig. 1C). We were unable to pick up low levels of ICx-induced NET release compared to medium control, which was indeed the case for PMA-induced NET release (Fig. 1D). Of note, similar results were obtained when using Picogreen and Sytox green fluorescence measurements on supernatants of these conditions (data not shown). In-depth exploration to improve visualization of NETs, we noted that NETs were topologically superimposed on the neutrophils: Fig. 1E illustrates that by using stacked imaging, neutrophils were found attached to the bottom of a well while released NETs were predominantly observed on top of the neutrophils. Comparing NET quantification, we demonstrated a significant higher result for ICx-induced NET release in three-dimensional (3D) imaging (mean NET area ± SEM: 1.03 ± 0.11) as compared to 2D imaging (mean NET area ± SEM: 0.04 ± 0.01, $p = 0.01$) (Fig. 1F). Altogether, sensitivity to quantify low levels of NETs upon ICx stimulation was increased by visualizing NET release 3-dimensionally (3D).

3.2. Automatization of 3D CSLM image acquisition

Because ICx induced NETs in fewer neutrophils as compared to PMA, we aimed to further augment the sensitivity of the NET quantification assay by increasing the total imaged surface to yield a higher number of neutrophils. By varying the fully automated image acquisition technique we showed that increasing number of HPFs and reducing the magnification led to larger image areas, correlating with a 10-fold increase of imaged neutrophils (Fig. 2A, B). When the 40× magnification was used, the area of the well captured is 2.8% when 25 HPFs were imaged, representing 194 ± 66 neutrophils (mean ± SEM). For optimal acquisition, 11.1% area of the well was captured when 25 HPFs were imaged with the 20× magnification, thereby analysing 1500 ± 247 neutrophils (mean ± SEM). We confirmed that imaging a larger well area by increasing the number of HPFs, resulted in a higher yield of neutrophils (Fig. 2C). To exclude observer subjectivity, 25 HPFs were captured in a constant pattern throughout each well, as illustrated in Fig. 2D. Captured images from 25 HPFs were stitched together to form one montage and 12 montages per well were mounted to form a 3D-image, which was used for digital image analysis (Fig. 2E and Supplemental movie). When performing image analysis, the amount of NET release is calculated by the total area of Sytox green (%), corrected for the amount of imaged cells calculated by the total area of PKH26 (%). The NET area per amount of imaged neutrophil is thus calculated by the total area of NETs (Sytox positive) divided by the amount of neutrophils, represented by the mean area of PKH26. Regardless of the induction of NETosis, we demonstrated that the total area of PKH26 (%) correlated significantly with neutrophil counts in unstimulated conditions ($r = 0.99$, $p < 0.0001$) and ICx-stimulated conditions ($r = 0.95$, $p < 0.0001$) (Fig. 2F, G). PKH staining is drastically decreased upon PMA stimulation (75% with 12.5 nM PMA) compared to ICx stimulation (34% with 12.5 μg/ml ICx) (Fig. 2H, I), suggesting increased neutrophil death and/or cell loss with PMA compared to ICx-induced NETosis.

3.3. High sensitivity quantification of ICx-induced NET release shows a ROS-independent process

Using the above-described high-sensitivity NET quantification assay, we confirmed its applicability by further investigating ICx-induced NET release (see Fig. 3). Low levels of ICx induced NET release (mean NET area per neutrophil ± SEM: 1.1 ± 0.5) were not significantly different when diphenyleneiodonium (DPI) was added (mean NET area per neutrophil ± SEM: 0.8 ± 0.2, $p > 0.05$). PMA induced large amounts of NET release (mean NET area per neutrophil ± SEM: 107 ± 5.8) which was almost completely inhibited by DPI (mean NET area per neutrophil ± SEM: 2.9 ± 0.0, $p < 0.005$). Fig. 3B confirmed these findings in cross-sectional overviews of 3-dimensional images of each condition with and without DPI. Overall, these findings indicate that human ICx induce NETs in a ROS-independent manner.

3.4. RA and SLE serum samples show NET-inducing capability compared to normal human serum

To further confirm applicability of this assay in the analysis of NET release in ICx-mediated autoimmune diseases, we next used this assay to quantify NET release induced by serum of patients with rheumatoid arthritis (RA) and systemic lupus erythematosus (SLE). The mean NET area ± SEM per imaged neutrophil upon induction with RA serum was 0.46 ± 0.08, 0.69 ± 0.18 for SLE and 0.12 ±

0.06 for the NHS control (Fig. 4A). For RA, 18 out of 27 serum samples (67%) showed increased NET-inducing capacity compared to the NHS control and in SLE, 17 out of 20 samples (85%) showed increased NET-inducing capacity (Fig. 4B).

4. Discussion

The present study describes a novel method for automatic and highly sensitive quantification of NET release based on CLSM. With this assay,

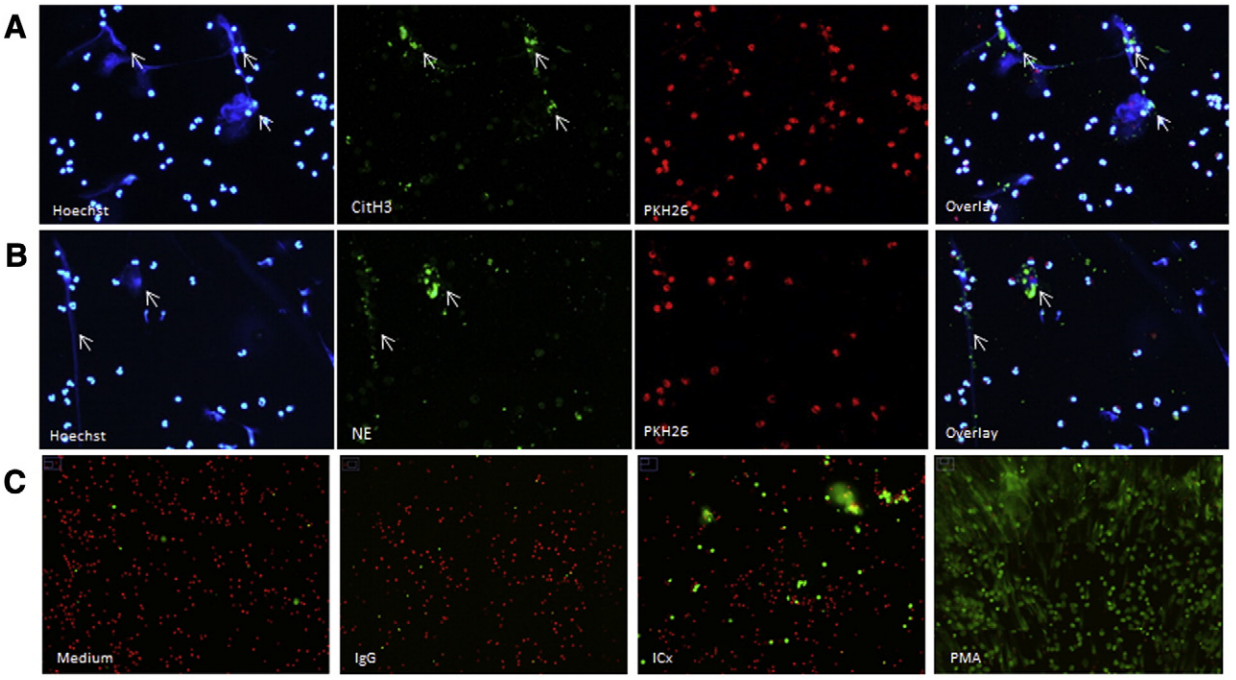

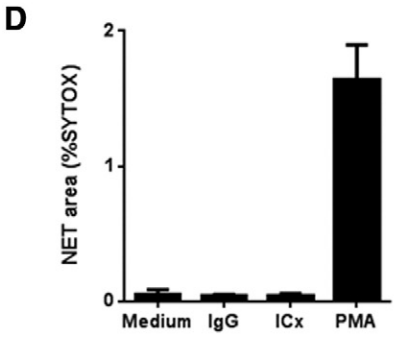

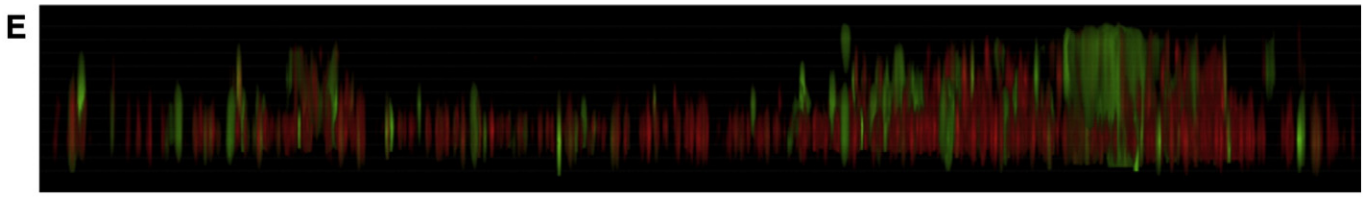

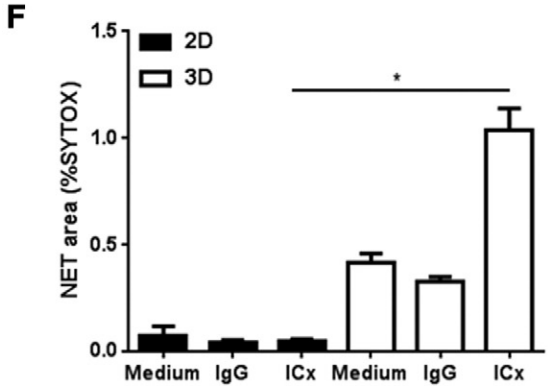

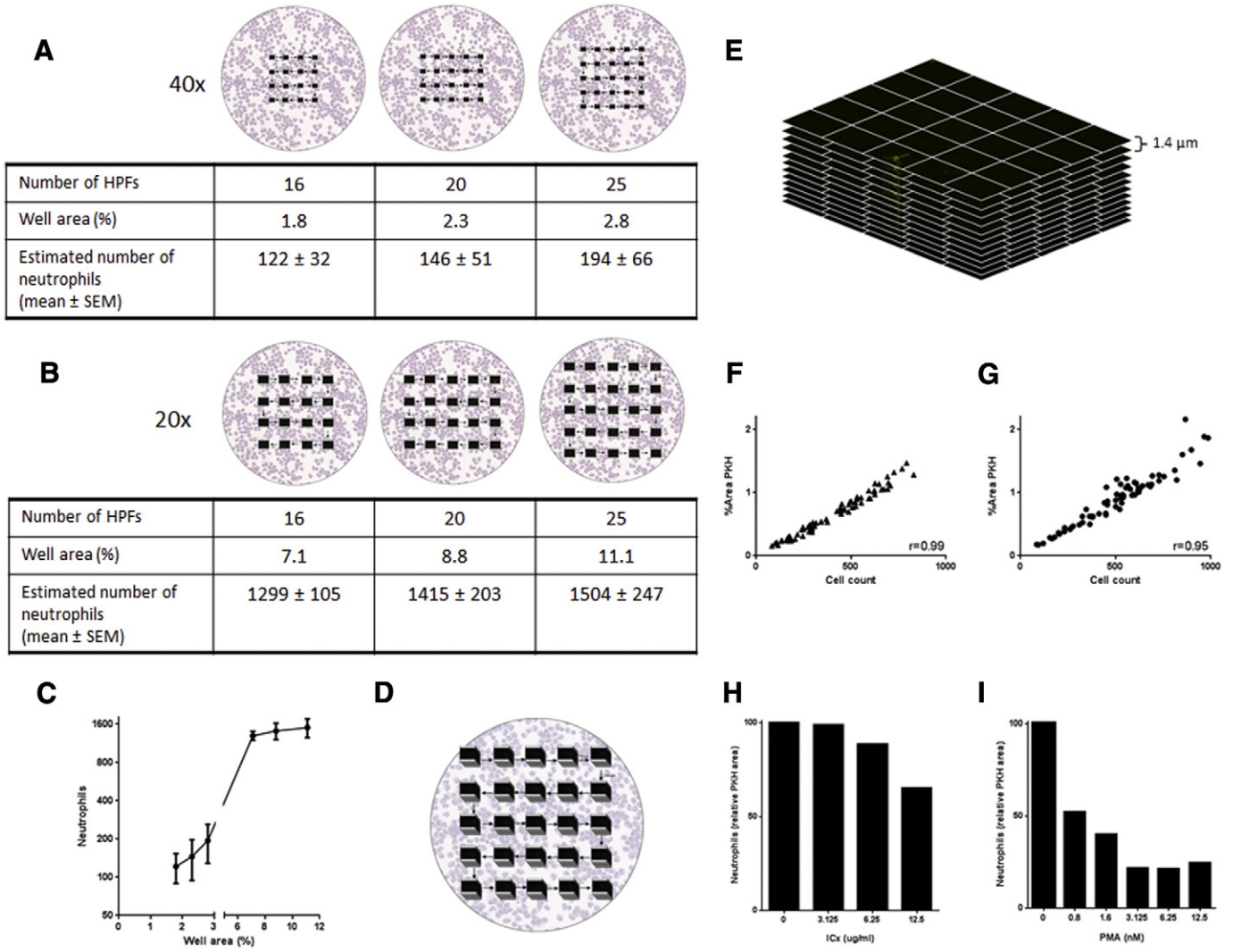

Fig. 2. Automatization of 3D CSLM image acquisition. The yield of (potentially netting) neutrophils is augmented by increasing the area per well imaged. (A) At a 40× magnification, 3D CSLM is capable of automatically imaging up to 2.8% of each well area. (B) At a 20× magnification, 3D CSLM is capable of automatically imaging up to 11.1% of each well area. (C) Depicted is the total amount of imaged neutrophils correlated to the imaged well area. Mean ± SEM are shown. (D) Thus, optimal yield was achieved by automatically capturing a fixed pattern 25 high power fields (HPFs) images for each well. (E) For image analysis, 25 HPF images are merged to one montage resulting in a total of 12 montages for each well suitable for digital image analysis. (F) When capturing high numbers of neutrophils, the percentage area of PKH26 correlates significantly with the amount of imaged neutrophils (unstimulated). (G) This correlation is preserved even after ICx-induced NET release (ICx 12.5 μg/ml). Seventy-two montages were analysed. (H, I) Relative in vitro neutrophil cell loss after ICx-induced NET release is lower compared to PMA-induced NETosis. The amount of neutrophil was quantified by percentage area of PKH26 positivity. Depicted is the relative reduction in percentage area.

we were able to demonstrate that the NET release upon stimulation with human heat-aggregated IgG immune complexes is independent of ROS production. Moreover, we show the applicability of this assay to quantify NET-inducing capacity in sera from RA and SLE patients.

The hallmark of the current method is its high sensitivity, which is based on two novel assay features. First, we introduced for the first time 3D imaging in a NET quantification assay. Since we observed that NETs are superimposed on neutrophils, we developed a more reliable detection of NETs by obtaining 12 z-stack images. Thus, we were able to demonstrate that low levels of NET release could be detected with 3D but not with 2D imaging. Second, the acquisition of (potentially netting) neutrophils is increased by imaging 11% of the total well area. In comparison, conventional methods based on fluorescence microscopy quantify 5–10 HPFs at 40× magnification correlating with an image area of 0.5–1% of each well [22,23]. The automated quantification method developed by Brinkmann obtained 5% of each well area by capturing 5 images randomly spread throughout the well with a 10× magnification [16]. When increasing the imaged area, we also show that an increased number of neutrophils is captured. Because the amount of measured NET release is directly related to the number of neutrophils captured in each HPF, we validated that PKH26 matched with the large number of neutrophils imaged. Of note, it is important to realize

Fig. 1. Human immune complexes (ICx) induce low level NET release detectable with three-dimensional CSLM. (A) PKH26-positive (red) neutrophils incubated with human ICx release extracellular DNA detected by Hoechst (blue) which are positive for the NET-specific marker citrullinated histon3 (citH3 — green) and, (B) the NET-specific marker neutrophil elastase (NE — green). Staining is representative of 3 separate experiments. (C) The amount of NET release is visually lower compared to PMA-stimulated NET release. PKH-labelled (red) neutrophils were stimulated for 4 h with either 12.5 μg/ml ICx or 12.5 nM PMA and NETs were stained with Sytox (green). Medium and the corresponding IgG concentration were taken along as controls. Subsequently, a montage image consisting of 25 high power fields (HPFs) was taken with confocal microscopy of which a part is shown here. (D) Low level NET release induced by ICx is not detected when quantified with the % area of positive Sytox staining. (E) Cross-sectional overview of a 3-dimensional image using 12 z-stacks demonstrated that NETs (green) are topologically superimposed on neutrophils (red). (F) Quantification of NETs by percentage area of Sytox green positive DNA in a 3D z-stack image, yields significantly more NETs as compared to a single focus 2D image ($p < 0.05$ for ICx 12.5 μg/mL). Bars represent mean ± SEM. *$p < 0.05$. Results are representative for three experiments.

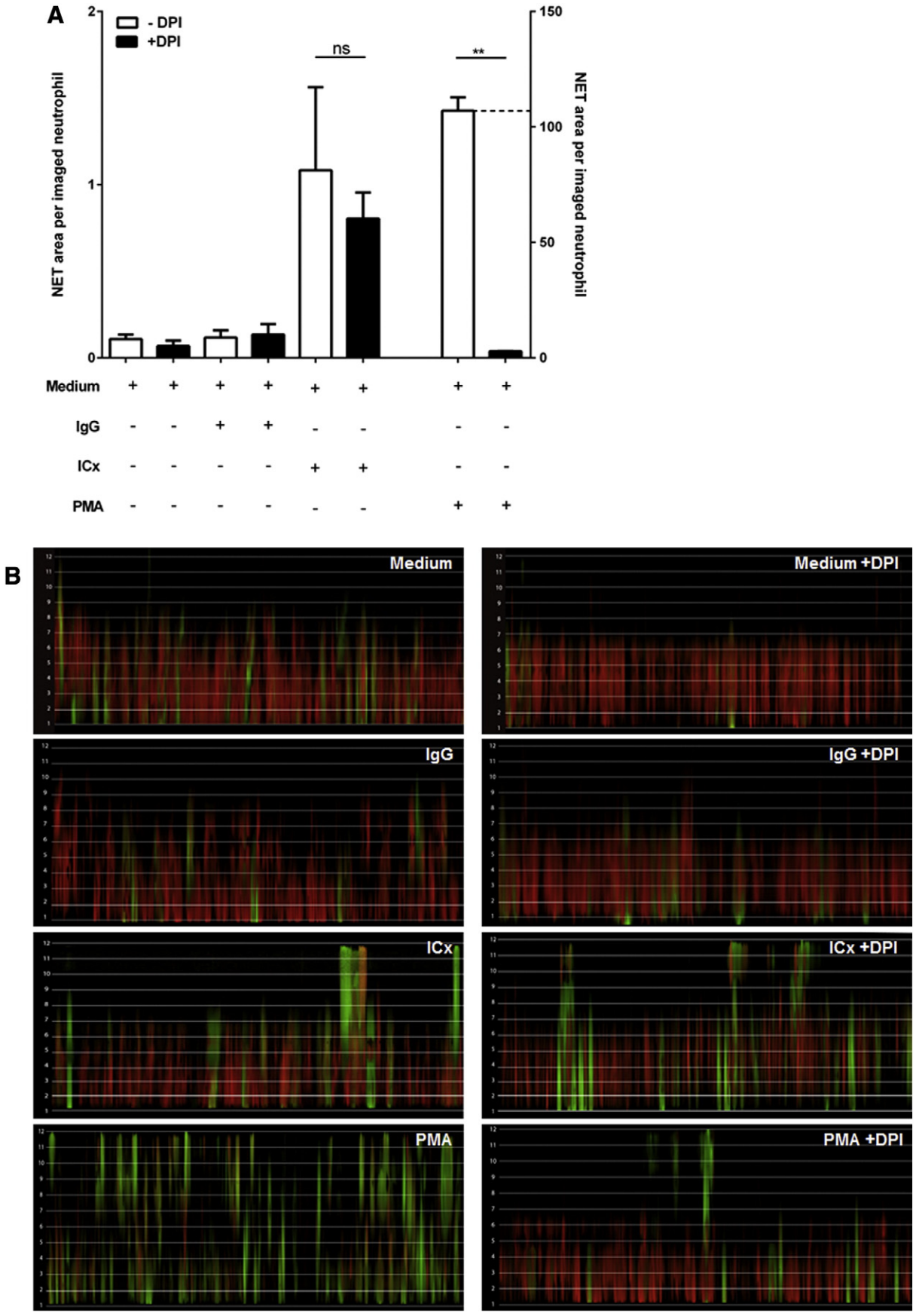
A
- DPI
+DPI
ns
**
NET area per imaged neutrophil
NET area per imaged neutrophil
2
1
0
150
100
50
0
Medium + + + + + + + +
IgG - - + + - - - -
ICx - - - - + + - -
PMA - - - - - - + +
B
Medium
Medium +DPI
IgG
IgG +DPI
ICx
ICx +DPI
PMA
PMA +DPI

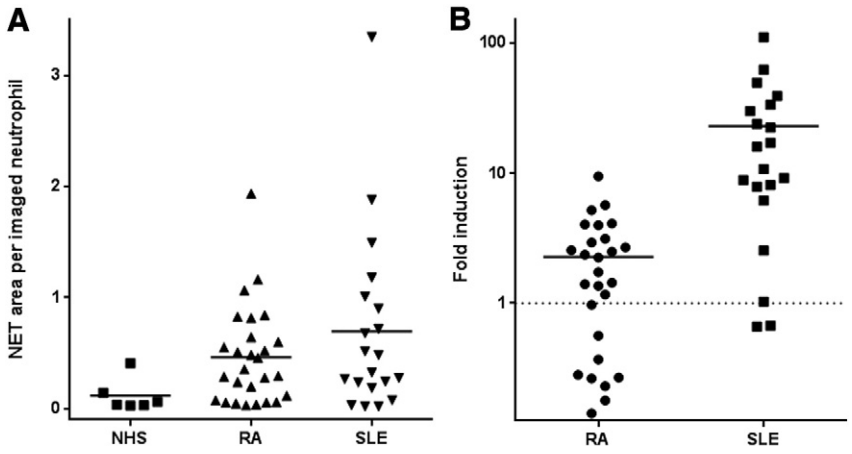

Fig. 4. Quantification of NET release induced by RA and SLE serum. (A) NET release was measured upon induction with 10% serum from 27 RA patients, 20 SLE patients and 6 NHS controls. (B) The amount of NET release upon stimulation with RA and SLE serum is shown relative to the NHS control (fold induction). The NHS control value is based on three different NHS samples used per experiment. The fold induction was calculated relative to the mean NHS value within the same experiment. All samples were tested in triplicate. NET release is induced in 18 out of 27 RA samples and in 17 out of 20 SLE samples. Each sample is represented by one dot or cube.

that the current assay includes limited pipetting steps, since no antibody stainings are used. Taken together, this novel assay has a significantly increased yield of NET detection, due to an increased sensitivity as compared to the currently reported assays to quantify NET release.

Quantifying NETs by immunofluorescence microscopy is inherently associated with observer subjectivity when images are acquired. To address this issue, we automated image acquisition which made it possible to capture 300 HPFs (25 HPFs in 12 z-stacks) for each well and, additionally, eliminate observer subjectivity and inter-observer variability during image acquisition. As a consequence, to handle the large image data sets, we semi-automated the digital image analysis. Thus, in contrast to previous NET quantification methods, we were able to identify a major reduction in PKH staining upon stimulation with PMA. This is most likely a result of general neutrophil death through NETosis induced by PMA. Importantly, neutrophil cell loss by NETosis was much smaller upon incubation with ICx illustrative of a quantitatively and qualitatively different process compared to PMA. Collectively, automated image acquisition of large areas from each well increased sensitivity while reducing observer subjectivity when quantifying NET release.

An important advantage of this assay is that it is compatible with the use of human IgG immune complexes. Previous reports investigating NET induction by ICx studied non-human ICx, such as soluble BSA/rabbit anti-BSA ICx [21] or immobilized HSA/rabbit polyclonal anti-HSA ICx [13]. Until now, it was a common problem to measure human ICx-induced NET release in a Sytox green fluorescence assay (data not shown) or with Picogreen DNA measurements due to the interference of human IgG with the detection method [18]. Another complication is the lack of sensitivity of previous conventional methods. To our knowledge, this is the first assay using a fully humanized system for NET quantification with human ICx.

There are a few limitations to this assay. First of all, inter-assay variability is present since the optimal imaging settings (e.g. exposure time) and analysis settings (e.g. intensity threshold) can vary between experiments. The use of different neutrophil donors is an uncontrollable variable that could add to inter-assay variability. Another limitation is the use of the specific dyes PKH26 and Sytox. A more specific NET marker could improve the assay's specificity for NETs. However, as yet, the current available NET-specific stainings such as citrullinated histone and neutrophil elastase have a low sensitivity and would therefore reduce the current assay's sensitivity to detect low levels of extracellular DNA [24,25]. Future investigations will attempt to further reduce assay variability and decrease duration of image acquisition.

The applicability of this method was first established in our experiments characterizing human ICx-induced NET release. By using DPI, which inhibits NADPH oxidase and ROS production, we demonstrated that ICx induction of (low levels of) NET release was different from PMA-induced (high levels of) NET release. This observation was in accordance with a previous report showing that soluble BSA/anti-BSA ICx-induced NET release is independent on the formation of ROS [21]. Moreover, we show the ability of this assay to quantify NET release upon stimulation with sera from RA and SLE patients. Compared to the NHS control, RA and SLE sera show increased capability to induce NET release. To minimize the potential inter-assay variability, the NET-inducing capacity is shown relative to the NHS control used in the corresponding experiment as well in Fig. 4B. In summary, we could successfully quantify the NET-inducing capacity of RA and SLE sera. Further investigations will focus on the NET-inducing capacity of multiple AID samples and factors involved in NET release in AID.

In conclusion, we have described a novel method to quantify NET release in vitro by applying a semi-automated 3D CLSM image analysis. This assay has four advantages over the currently reported, conventional methods for NET quantification: 1) the assay has increased sensitivity to detect low levels of NETs; 2) the assay is semi-automated minimizing observer variability; 3) the assay is performed in a fully humanized system; 4) the assay allows high-throughput analysis. With this novel method we were able to detect NET release induced by RA and SLE serum samples with high sensitivity. Future investigations will aim to apply this assay in order to investigate the ability of circulating factors to induce NET release in autoantibody-mediated diseases, such as ANCA-associated vasculitis, SLE, rheumatoid arthritis, antiphospholipid syndrome and cryoglobulinemic vasculitis.

Supplementary data to this article can be found online at http://dx.doi.org/10.1016/j.autrev.2016.02.018.

Fig. 3. High sensitivity quantification of ICx-induced NET release is ROS-independent. (A) NADPH-oxidase was inhibited through pre-incubation of neutrophils with 1 μM diphenyleneiodonium (DPI) and subsequently NETs were induced with human IgG (6.25 μg/ml), ICx (6.25 μg/ml) and PMA (25 nM) or medium (unstimulated control). ROS-inhibition did not influence ICx-induced NET release, plotted on the left y-axis, whereas PMA-induced NET release, plotted on the right y-axis, was almost completely blocked. ns = not significant, $^{**}p < 0.005$. (B) Corresponding cross-sectional overview of a 3-dimensional images using 12 z-stacks illustrating ICx-induced NET release is ROS independent. Results are representative for three experiments. Bars represent mean ± SEM.

Take-home messages

- We developed a highly sensitive method for the detection and quantification of low level neutrophil extracellular trap (NET) release.
- This novel method was successfully applied for the quantification of the NET-inducing capacity of human immune complexes and sera from rheumatoid arthritis and systemic lupus erythematosus patients.

Conflict of interest

T.K., T.J.R., C.K and Y.K.O.T are inventors of the UK patent application No. 1517458.4 dealing with the assay to quantify extracellular traps.

Funding

The work of Tineke Kraaij and Y.K. Onno Teng was supported by the Dutch Kidney Foundation (KJPB12.028) and a Clinical Fellowship by the Netherlands Organisation for Scientific Research (project no. 90713460).

Acknowledgements

We thank Maarten van der Linden and prof. Linde Meyaard from the Division Laboratory and Pharmacy, Laboratory of Translational Immunology, Department of Immunology at the University Medical Center Utrecht for sharing their expertise and critical comments on this project.

References

[1] Pilsczek FH, Salina D, Poon KKH, Fahey C, Yipp BG, Sibley CD, et al. A novel mechanism of rapid nuclear neutrophil extracellular trap formation in response to *Staphylococcus aureus*. J Immunol 2010;185:7413–25. http://dx.doi.org/10.4049/jimmunol.1000675.

[2] Brinkmann V, Reichard U, Goosmann C, Fauler B, Uhlemann Y, Weiss DS, et al. Neutrophil extracellular traps kill bacteria. Science 2004;303(80-):1532–5. http://dx.doi.org/10.1126/science.1092385.

[3] Urban CF, Ermert D, Schmid M, Abu-Abed U, Goosmann C, Nacken W, et al. Neutrophil extracellular traps contain calprotectin, a cytosolic protein complex involved in host defense against *Candida albicans*. PLoS Pathog 2009;5, e1000639. http://dx.doi.org/10.1371/journal.ppat.1000639.

[4] McCormick A, Heesemann L, Wagener J, Marcos V, Hartl D, Loeffler J, et al. NETs formed by human neutrophils inhibit growth of the pathogenic mold *Aspergillus fumigatus*. Microbes Infect 2010;12:928–36. http://dx.doi.org/10.1016/j.micinf.2010.06.009.

[5] Lande R, Gregorio J, Facchinetti V, Chatterjee B, Wang Y-H, Homey B, et al. Plasmacytoid dendritic cells sense self-DNA coupled with antimicrobial peptide. Nature 2007;449:564–9. http://dx.doi.org/10.1038/nature06116.

[6] Kessenbrock K, Krumbholz M, Schönermarck U, Back W, Gross WL, Werb Z, et al. Netting neutrophils in autoimmune small-vessel vasculitis. Nat Med 2009;15:623–5. http://dx.doi.org/10.1038/nm.1959.

[7] Nakazawa D, Shida H, Tomaru U, Yoshida M, Nishio S, Atsumi T, et al. Enhanced formation and disordered regulation of NETs in myeloperoxidase-ANCA-associated microscopic polyangiitis. J Am Soc Nephrol 2014;1–8. http://dx.doi.org/10.1681/ASN.2013060606.

[8] Garcia-Romo GS, Caielli S, Vega B, Connolly J, Allantaz F, Xu Z, et al. Netting neutrophils are major inducers of type I IFN production in pediatric systemic lupus erythematosus. Sci Transl Med 2011;3:73ra20. http://dx.doi.org/10.1126/scitranslmed.3001201.

[9] Lande R, Ganguly D, Facchinetti V, Frasca L, Conrad C, Gregorio J, et al. Neutrophils activate plasmacytoid dendritic cells by releasing self-DNA-peptide complexes in systemic lupus erythematosus. Sci Transl Med 2011;3:73ra19. http://dx.doi.org/10.1126/scitranslmed.3001180.

[10] Khandpur R, Carmona-Rivera C, Vivekanandan-Giri A, Gizinski A, Yalavarthi S, Knight JS, et al. NETs are a source of citrullinated autoantigens and stimulate inflammatory responses in rheumatoid arthritis. Sci Transl Med 2013;5:178ra40. http://dx.doi.org/10.1126/scitranslmed.3005580.

[11] Hakkim A, Fürnrohr BG, Amann K, Laube B, Abed UA, Brinkmann V, et al. Impairment of neutrophil extracellular trap degradation is associated with lupus nephritis. Proc Natl Acad Sci U S A 2010;107:9813–8. http://dx.doi.org/10.1073/pnas.0909927107.

[12] Leffler J, Martin M, Gullstrand B, Tydén H, Lood C, Truedsson L, et al. Neutrophil extracellular traps that are not degraded in systemic lupus erythematosus activate complement exacerbating the disease. J Immunol 2012;188:3522–31. http://dx.doi.org/10.4049/jimmunol.1102404.

[13] Behnen M, Leschczyk C, Moller S, Batel T, Klinger M, Solbach W, et al. Immobilized immune complexes induce neutrophil extracellular trap release by human neutrophil granulocytes via Fc RIIIB and Mac-1. J Immunol 2014;193:1954–65. http://dx.doi.org/10.4049/jimmunol.1400478.

[14] Guimarães-Costa AB, Nascimento MTC, Froment GS, Soares RPP, Morgado FN, Conceição-Silva F, et al. *Leishmania amazonensis* promastigotes induce and are killed by neutrophil extracellular traps. Proc Natl Acad Sci U S A 2009;106:6748–53. http://dx.doi.org/10.1073/pnas.0900226106.

[15] Van Avondt K, Fritsch-Stork R, Derksen RHWM, Meyaard L. Ligation of signal inhibitory receptor on leukocytes-1 suppresses the release of neutrophil extracellular traps in systemic lupus erythematosus. PLoS One 2013;8, e78459. http://dx.doi.org/10.1371/journal.pone.0078459.

[16] Brinkmann V, Goosmann C, Kühn LI, Zychlinsky A. Automatic quantification of in vitro NET formation. Front Immunol 2012;3:413. http://dx.doi.org/10.3389/fimmu.2012.00413.

[17] Coelho LP, Pato C, Friães A, Neumann A, von Köckritz-Blickwede M, Ramirez M, et al. Automatic determination of NET (neutrophil extracellular traps) coverage in fluorescent microscopy images. Bioinformatics 2015;31:2364–70. http://dx.doi.org/10.1093/bioinformatics/btv156.

[18] Invitrogen. Quant-iT™ PicoGreen® dsDNA reagent and kits; 2008 1–7.

[19] Lems-Van Kan P, Verspaget HW, Peña AS. ELISA assay for quantitative measurement of human immunoglobulins IgA, IgG, and IgM in nanograms. J Immunol Methods 1983;57:51–7. http://dx.doi.org/10.1016/0022-1759(83)90064-9.

[20] Lood C, Blanco LP, Purmalek MM, Carmona-Rivera C, De Ravin SS, Smith CK, et al. Neutrophil extracellular traps enriched in oxidized mitochondrial DNA are interferogenic and contribute to lupus-like disease. Nat Med 2016;1–11. http://dx.doi.org/10.1038/nm.4027.

[21] Chen K, Nishi H, Travers R, Tsuboi N, Martinod K, Wagner DD, et al. Endocytosis of soluble immune complexes leads to their clearance by FcyRIIIB but induces neutrophil extracellular traps via FcyRIIA in vivo. Blood 2012;120:4421–31. http://dx.doi.org/10.1182/blood-2011-12-401133.

[22] Tanaka K, Koike Y, Shimura T, Okigami M, Ide S, Toiyama Y, et al. In vivo characterization of neutrophil extracellular traps in various organs of a murine sepsis model. PLoS One 2014;9, e111888. http://dx.doi.org/10.1371/journal.pone.0111888.

[23] Yipp BG, Petri B, Salina D, Jenne CN, Scott BNV, Zbytnuik LD, et al. Infection-induced NETosis is a dynamic process involving neutrophil multitasking in vivo. Nat Med 2012;18:1386–93. http://dx.doi.org/10.1038/nm.2847.

[24] Zhao W, Fogg DK, Kaplan MJ. A novel image-based quantitative method for the characterization of NETosis. J Immunol Methods 2015. http://dx.doi.org/10.1016/j.jim.2015.04.027.

[25] Ciepiela O, Ostafin M, Bystrzycka W, Sieczkowska S, Moskalik A, Demkow U, et al. Flow cytometric quantification of neutrophil extracellular traps: limitations of the methodological approach. Am J Hematol 2015. http://dx.doi.org/10.1002/ajh.24257.